

# Seismic resistance of reinforced embankment by model shaking table tests

Y.Koga, Y.Ito, S.Washida & T.Shimazu

Public Works Research Institute, Ministry of Construction, Japan

**ABSTRACT:** It was shown from 14 cases of model shaking table tests of embankments reinforced with nonwoven fabrics, plastic nets and steel bars, that the seismic resistance of an embankment is increased if a reinforcing element of high tensile stiffness is used to anchor the embankment to the bed slope. The local failure of the fill slope surface must also be prevented by an appropriate protection work. Moreover, the damage degree of embankments agreed well with calculation results by a circular slip surface method which considers the effect of the tensile force of reinforcing element.

## 1. INTRODUCTION

Reinforcing embankments with geotextile or steel plates, etc. has recently attracted wide interest. The evaluation of the effect of geotextile or other reinforcing elements on the seismic resistance of embankments is an important issue in such a country with high seismicity as Japan. This paper presents a seismic effect of reinforcement with geotextile and steel bar on the embankments constructed on an inclined ground by a series of model shaking table tests and their stability analyses (Koga et al., 1988).

## 2. MODEL SHAKING TABLE TEST

### 2.1 Models

Fig. 1 shows an example of cross section of test models. Each model consists of a bed slope and a fill part on it. The model was made in a steel box of 8 m long, 2 m high and 1 m wide. Both side slopes of one model were made in different conditions and two cases were simultaneously tested using one model. As summarized in Table 1, 7 models with 14 cases were so far tested.

Following conditions were varied in each case : slope surface gradient, existence of benches on a bed slope, kind of reinforcing element, reinforcement spacing, slope protection, etc.

The bed slope was made of wet sandy silt (ML,  $w = 19\%$ ) sufficiently compacted by a wooden block so as to be stable against vibration. The fill part was made of air dried sand (SP,  $w = 6-12\%$ ) which was compacted to a relative density of about 50% by human foot. Reinforcing elements were nonwoven fabrics, plastic nets and steel bars. These properties are described in Table 2. Nails, 15 cm long, were used to fix nonwoven fabrics and plastic nets to the bed

slopes. Steel bars were penetrated by 30 cm to the bed slope. The overlapped length of nonwoven fabrics and plastic nets were 30 cm irrespective of the spacing.

A following scaling law was adopted; the reinforcement ratio  $R$  defined by the following equation is same for prototype and model assuming the Poisson's ratio  $\nu = 0$  for reinforcing elements (Tatsuoka et al., 1985).

$$R_f = \frac{-\epsilon_{3R} \cdot E \cdot t}{\sigma_{3R} \cdot \Delta H} \quad (1)$$

where  $\epsilon_{3R}$  = average horizontal tensile strain of the reinforced soil ( $\epsilon_{3R} < 0$ );  $E$  = Young's modulus of the reinforcing element;  $t$  = thickness of the reinforcing element;  $\sigma_{3R}$  = horizontal confining pressure;  $\Delta H$  = spacing of the reinforcing element.

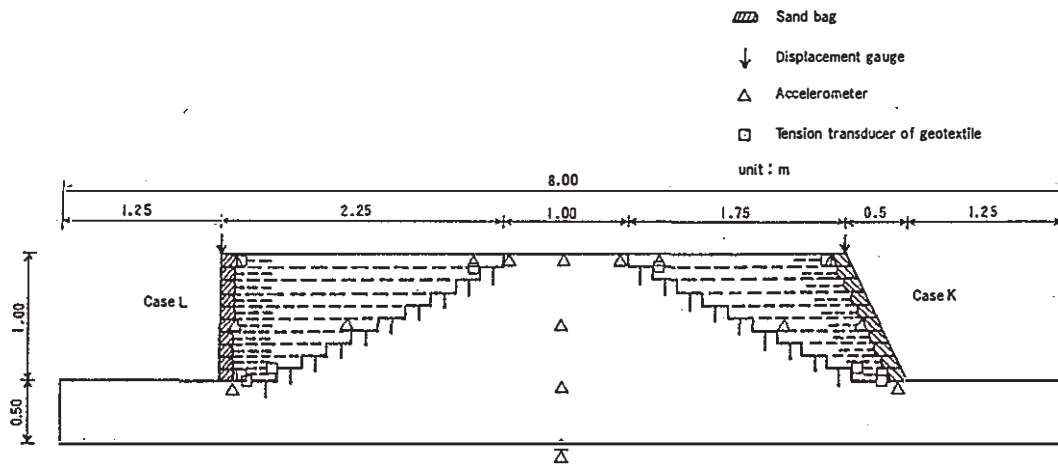
This reinforcement ratio represents the ratio of strength increase of a reinforced soil to an unreinforced one at a specified reference strain. The reinforcing element was chosen so that the model scale was to be 1/7 to the prototype.

### 2.2 Excitation conditions and measurement

Excitation was conducted under sinusoidal wave loading of 4Hz and 10 sec. Excitation acceleration was increased step by step ranging from 100 to 800 gal. The shaking table was stopped for each excitation level and the damage degree was observed and horizontal and vertical displacements of the observation marks were measured. The acceleration, settlement and tensile force of nonwoven fabrics and steel bars were recorded during the excitation. Moreover the overall deformation of the model was observed by taking photos of drawn meshes with coloured sands in front surface of the model.

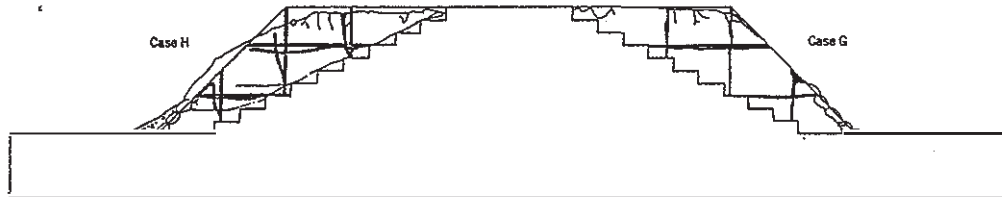
### 2.3 Test results

Fig.2 shows the overall deformation of the model 4.



Model 6 (Case K, L)

Fig.1 Example of Test Models



Model 4 (Case G, H) after 700gal excitation

Fig 2 Deformation after Excitation

Table 1 Test Model

Name of embankments (case)	Model	Kinds of reinforcing elements	Reinforcement spacing	Anchorage to bed slope	Overlapping	Slope gradient	Sand bag on slope surface	Water content (%)
A	1	R None	—	—	—	1 : 1.5	—	11.5
B		L Nonwoven fabrics	10cm	No	No	1 : 1.5	No	11.3
C	2	R None	—	—	—	1 : 1.5	—	9.3
D		L Nonwoven fabrics	10cm	Yes	No	1 : 1.5	No	10.1
E	3	R None	—	—	—	1 : 1	—	8.1
F		L Nonwoven fabrics	10cm	No	Yes	1 : 1	Yes	7.8
G	4	R do	10cm	Yes	Yes	1 : 1	Yes	6.3
H		L do	20cm	Yes	Yes	1 : 1	Yes	6.5
I	5	R Reinforcing bar	Horizontally 10cm Vertically 20cm	Penetrated by 30cm	—	1 : 1	—	6.3
J		L Plastic nets	20cm	Yes	Yes	1 : 1	Yes	6.5
K	6	R Nonwoven fabrics	10cm	Yes	Yes	1 : 0.5	Yes	8.3
L		L do	10cm	Yes	Yes	1 : 0	Yes	8.4
M	7	R None	—	—	—	1 : 1	—	15.2
N		L Nonwoven fabrics	10cm	Yes	Yes	1 : 1	Yes	15.4

Table 2 Properties of Reinforcing Elements

Kinds	Properties
Nonwoven fabrics	Nylon 70%, Polyester 30%, Thickness 0.2mm
Plastic net	Polyethylene 100%, Grid 2.5×2.5mm
Steel bar	Pianowire, diameter 3.5mm

after the excitation of 700 gal as an example of test results. When a model embankment was excited under such a large acceleration, it slid along a slip surface and its crest settled. Such a figure shows the damage mode and feature of each embankment model.

Fig.3. shows a relationship of a cumulative crest settlement and an excitation acceleration.

The damage features of reinforced embankments are summarized as follows.

1) Unreinforced embankments slipped near the boundary to the bed slope. Reinforced ones with slope surface gradients of 1:1.5 and 1:1.0 also deformed relatively largely near the above boundary, however, the deformation was smaller than that of unreinforced ones. The deformed region was in a shallower part for the reinforced one with steeper slope gradients.

2) The deformation of reinforced embankments were less than unreinforced ones for the same slope gradient (Fig.3(a)).

3) As the spacing of nonwoven fabrics becomes smaller, the crest settled less (Fig.3(a)).

4) An embankment reinforced with plastic nets, whose tensile stiffness is larger, settled less than one reinforced with nonwoven fabrics in the same spacing (Fig.3(a)).

5) Embankments settled and deformed less when the nonwoven fabrics were fixed to the bed slope (Fig.3(b)).

6) Embankments deformed less when nonwoven fabrics or plastic nets were overlapped to their slope surface (Fig.3(a)), however, the overlapped geotextiles were pulled out during a large vibration at the upper layer where the overburden pressure was small.

7) As the slope got steeper, the deformation of the reinforced and unreinforced embankments became larger, however, the tendency of deformation increase of the reinforced ones was assumed rather smaller (Fig.3(c)).

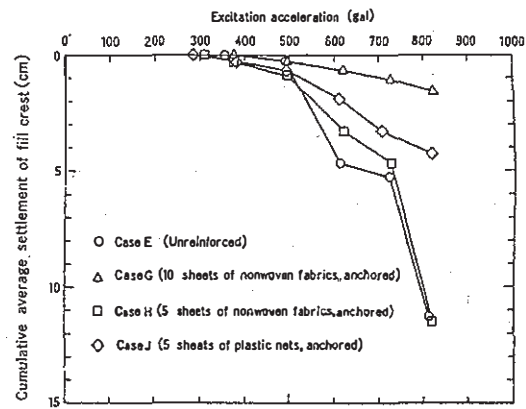
8) Penetrated steel bars showed an effect to decrease the settlement of the embankment. However, its effect was not enough because the shallow part of the slope was removed when the slope protection was not effective. It suggests that steel bars must be connected to the slope protection works so that the embankment be effectively reinforced.

### 3. STABILITY ANALYSIS

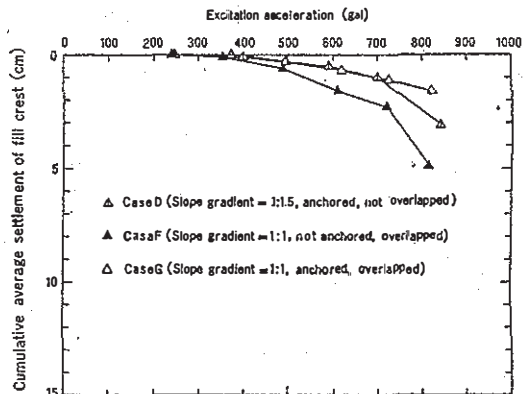
#### 3.1 Stability analysis method

A stability of a reinforced embankment must be investigated from various viewpoints because it can possibly fail in various modes. A stability of an unreinforced embankment is generally examined for its overall stability by a slip surface method. In the case of a reinforced embankment, not only the stability of an overall reinforced region, but such a local stability as a pulling out or a breakage of a reinforcing element and a bulging of soil of a slope surface must be examined.

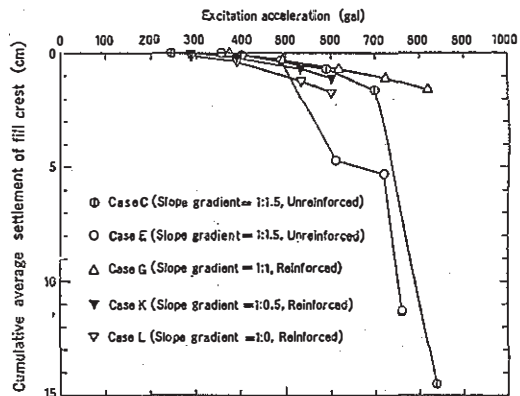
The main failure mode of the embankment in these tests was that the fill slipped near the boundary to the bed slope and not that reinforcing elements were pulled out or broken apart. Therefore it was presumed that not a small strain occurred in the reinforcing element. Consequently it was considered important to



(a) Effect of Reinforcement, Spacing and Material (Slope gradient = 1:1)



(b) Effect of Anchorage and Overlapping (10 sheets of nonwoven fabrics)



(c) Effect of Slope Gradient (Unreinforced and reinforced with anchored 10 sheets of nonwoven fabrics)

Fig.3 Relationship between Excitation Acceleration and Cumulative Settlement of Fill crest

examine the overall failure of the embankment which was observed in the tests.

There is not yet an established method as a seismic stability analysis method of a reinforced embankment. Since a circular slip surface method with a seismic coefficient is frequently adopted for seismic stability analyses, it was extended as follows to include the effect of reinforcing element.

$$F_s = \frac{\sum R[c\ell + \{W \cdot \cos \alpha - k_h W \cdot \sin \alpha + T_r \cdot \sin(\alpha + \theta)\} \cdot \tan \phi]}{\sum [R \cdot W \cdot \sin \alpha + y \cdot k_h W \cdot \cos \alpha - R \cdot T \cdot \cos(\alpha + \theta)]} \quad (2)$$

where  $R$  = radius of a slip circle;  $c$  = cohesion of soil;  $\phi$  = friction angle of soil;  $W$  = self weight of a slice;  $\ell$  = length of an arc of a slice;  $b$  = width of a slice;  $k_h$  = horizontal seismic coefficient;  $y$  = vertical distance between the center of a circular arc and the center of gravity of a slice;  $T_r$  = tensile force of reinforcing element when the reinforced earth reaches a failure state;  $T$  = tensile force of reinforcing element acting on the sliding earth mass in equilibrium;  $\alpha, \theta$  = angles shown in Fig.4.

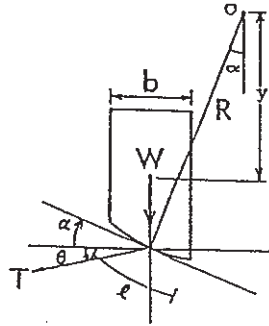


Fig.4 Slice for a Circular Slip Surface Analysis

The calculated factor of safety can be compared with that for unreinforced embankments, which enables to evaluate the stability increase by the reinforcement. Above equation is an extension of the Fellenius formula, which considers the effect of the tensile force of the reinforcing element to bind and to hold the sliding earth mass.

The characteristics of above equation is as follows.

The numerator of the equation to represent a resistant moment is obtained from a tensile force of the reinforcing element at failure, whereas the denominator of the equation to represent a sliding moment from a working tensile force in equilibrium. The tensile force of reinforcing element is determined from its tensile strain caused by the deformation of the surrounding soil, which was obtained so that the strain is compatible with shear strain of the soil along a failure surface (band) based on the following assumptions (see Fig.5).

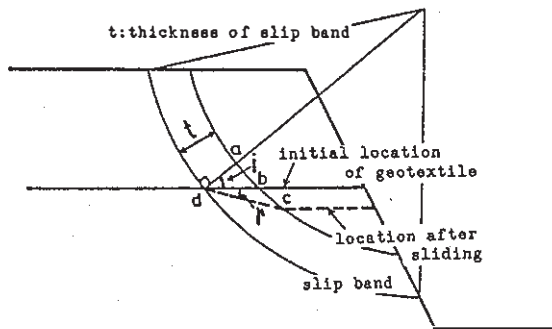


Fig.5 Calculation of Tension of Geotextile

1) A slip surface consists of a slip band with a constant thickness of a constant shear strain.

2) Reinforcing element deforms in a body with a soil therefore it cannot be separated from a soil.

3) The shear strain of the slip band generates a tensile strain of a reinforcing element intersecting the slip band.

4) The tensile strength of the reinforcing element is large enough to hold the slip of the earth mass.

As a consequence of these assumptions, the tensile strain of the reinforcing element  $\epsilon_s$  is given as below.

$$\epsilon_s = \frac{cd - bd}{bd} = \frac{\cos i - \cos(i + \gamma')}{\cos(i + \gamma')} \quad (3)$$

where  $i$  = angle between the reinforcing element and normal line to a slip surface;  $\gamma'$  = corrected shear strain of a soil, generally not equal to that of the slip band.

The working tensile force  $T$  of the reinforcing element of the sliding mass in equilibrium is provisionally calculated from the following equation by assuming the linear relationship between all the mobilized forces on the mass and the deformation of the mass (see Fig.6).

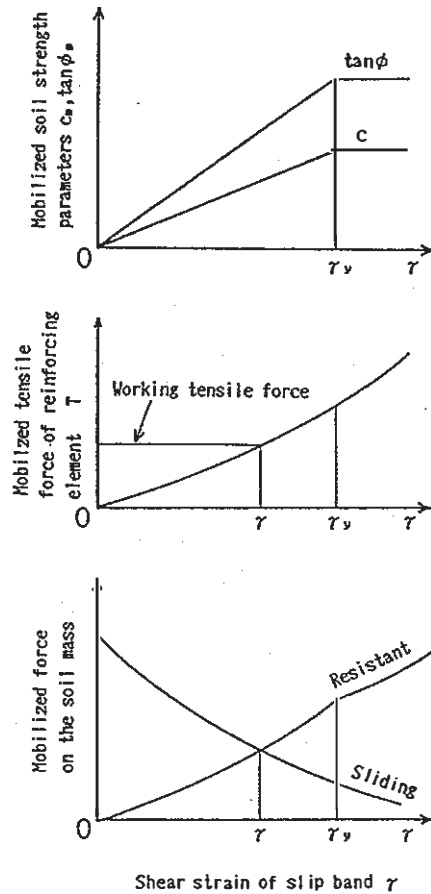


Fig.6 Relationship between Mobilized Force and Deformation of Soil Mass

$F_s=1$

$$= \frac{\sum R [c_m l + (W \cdot \cos \alpha - k_h W \cdot \sin \alpha + T \cdot \sin(\alpha + \theta)) \cdot \tan \phi_m]}{\sum [R \cdot W \cdot \sin \alpha + k_h W \cdot \cos \alpha - R \cdot T \cdot \cos(\alpha + \theta)]} \quad (4)$$

where  $c_m$  = mobilized cohesion of soil;  $\phi_m$  = mobilized friction angle of soil.

The linear relationship implies

$$\frac{c_m}{c} = \frac{\tan \phi_m}{\tan \phi} = \frac{\gamma}{\gamma_y} \quad (5)$$

where  $\gamma$  = shear strain of slip band;  $\gamma_y$  = shear strain of soil at failure.

### 3.2 Stability analysis conditions

Stability analyses were conducted on some of the test models changing the excitation accelerations.

The analyzed models were unreinforced embankments and reinforced ones whose reinforcing elements were fixed to the bed slope.

The unit weight, cohesion and friction angle of the fill used for the calculation were 1.56 tf/m<sup>3</sup>, 0.3 tf/m<sup>2</sup> and 33° respectively. It was assumed that the shear strength of the bed slope was large enough and no slip surface to cut the bed slope was considered. While the friction angle of the fill was obtained from a triaxial test the cohesion of the fill was obtained from a critical height of a vertical cut of a ground made in the same manner as that of shaking tests.

The formula was as follows.

$$c = \frac{\gamma_t H_c}{2.67} \tan \left( 45^\circ + \frac{\phi}{2} \right) \quad (6)$$

where  $\gamma_t$ : unit weight of ground;  $H_c$ : critical height.

The tensile stiffness of the reinforcing element to calculate a tensile force is shown in Table 2. The seismic coefficient was given based on the measured acceleration during shaking table tests.

### 3.3 Stability analysis results

Fig.7 shows a relationship between safety factors calculated from Eq.(2) and excitation acceleration.

The shear strain of 8% is taken as a failure criterion of an embankment on the basis of a triaxial compression test result, and the tensile force of the reinforcing element  $T_r$  was calculated to correspond with the above strain. Obviously no tensile force of the reinforcing element was considered for unreinforced embankments.

Fig.7(a) indicates the followings.

1) Among the embankments of a slope gradient of 1:1, the least factor of safety was obtained for an unreinforced embankment.

2) A little larger factors were obtained for the cases of 5 and 10 sheets of nonwoven fabrics.

3) The largest factor was obtained for that of 5 sheets of plastic nets.

4) The differences of safety factors among the unreinforced and 2 nonwoven fabrics-reinforced

embankments were slight, which indicates that the reinforcement effect by such a reinforcing element with a small tensile stiffness is small. Besides the plastic nets with a larger tensile stiffness gave fairly larger factors of safety.

Fig.7(b) shows that the safety factor of the unreinforced and reinforced embankments remarkably decreases as the slope gets steeper.

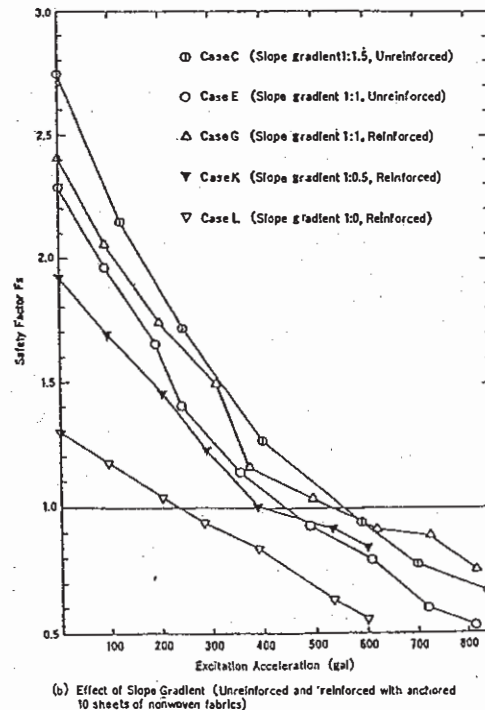
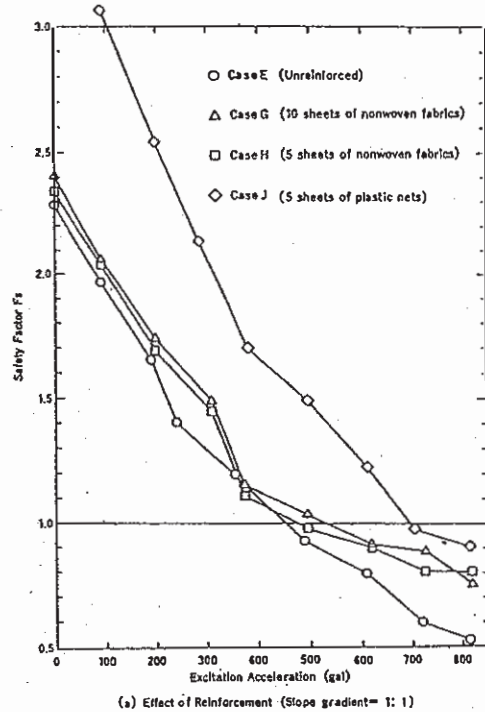


Fig.7 Relationship between Excitation Acceleration and Safety Factor

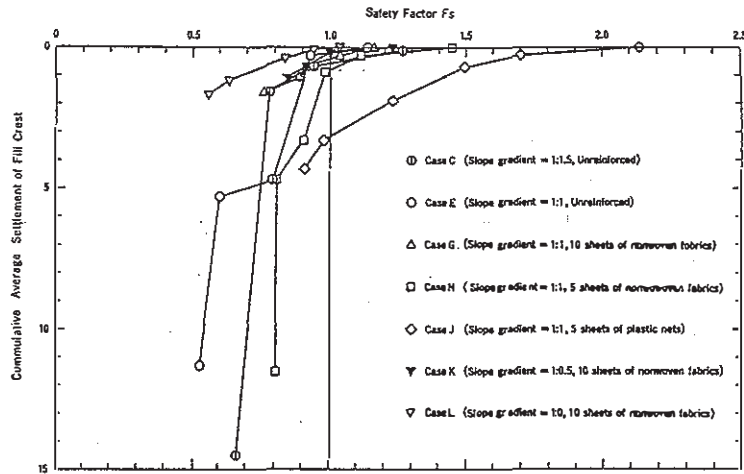


Fig.8 Relationship between Safty Factor and Measured Settlement

Fig.8 shows a relationship between a calculated safety factor and a cumulative settlement of a fill crest. In general, a fairly unique relationship with little scatter exists in Fig.8 except the case of a slope gradient of 1:0.5 and 1:0, and that of plastic nets, irrespective of the existence of reinforcing elements and reinforcement spacing. Moreover the settlement rapidly increases when  $F_s$  is less than from 0.95 to 1.0 in the case of nonwoven fabrics and a slope gradient of 1:1 and 1:1.5, which suggests the calculation method of Eq. (2) is useful for the assessment of a failure or deformation of a reinforced embankment whose slope surface is not so steep.

The reason that the calculated factor of safety is so small for the embankment of steep slope is because the safety factor is calculated by use of the Fellenius method which neglects the interslice force, which gives smaller safety factor than that with the above force, and also the Eq. (2) neglects the resistant effect of the overlapped geotextile slope facing and also the crest settlement of a steep slope becomes small against a certain strain of slip surface because the slip surface gets smaller as the slope gets steeper.

Followings are summarized from the above analysis results.

- 1) The calculation results by a circular slip surface method with a seismic coefficient method, which considers the binding and holding effect by a tensile force of reinforcing elements intersecting the slip surface, agreed well with the experimental results except the cases of steep slope.
- 2) It proved useful to calculate a tensile strain of a reinforcing element that is compatible with a shear deformation along a slip surface of an embankment to obtain a tensile force of a reinforcing element.

#### 4. CONCLUSION

- 1) Model shaking table tests of reinforced embankments with nonwoven fabrics, plastic nets and steel bars showed that a reinforced embankment has a fairly large seismic resistance if a reinforcing element with a large tensile stiffness is effectively fixed to a

bed slope. Besides the slope protection to prevent a local slope surface failure is also critical.

- 2) The degree of deformation of the embankment corresponded well to the calculation results by a circular slip surface method which considers the effect of tensile force of reinforcing element intersecting the slip surface except the cases of steep slope.

- 3) The selection of an appropriate slope protection works and the evaluation of its effect on the stability need a further research.

#### REFERENCES

- Koga, Y., et al. : Experimental Study on Seismic Resistance of Reinforced Embankment (in Japanese), Technical Memorandum of PWRI, 1988.3.
- Tatsuoka, F., et al. : Reinforcing of Cohesive-Soil-Embankment with Unwoven Fabric (in Japanese), Tsuchi-To-Kiso, JSSMFE, Vol.33, No.5, 1985.5.